 CMES, vol., no., pp.2-18,

The Influence of Crystal Surfaces on Dislocation Interactions in Mesoscopic Plasticity: A Combined Dislocation Dynamics- Finite Element Approach

R. Martinez[1] and N. M. Ghoniem[2]

Abstract: We focus here on the direct coupling of Dislocation Dynamics (DD) computer simulations with the Finite Element Method (FEM) to simulate plastic deformation of micro-scale structures, and investigate the influence of crystal surfaces on dislocation motion. A series of three-dimensional (3-d) DD simulations of BCC single crystals with a single shear loop in the (101)-[111] slip system are first presented. The purpose of these simulations is to explore the relationship between loop force distributions and the proximity of the loop to the crystal boundary. Traction boundary conditions on a single crystal model are satisfied through the superposition of the "image" stress field computed by FEM, and the elastic stress field of dislocations computed by DD. The force distribution on a prototypical shear loop is shown to consist of the superposition of Peierls, image, applied, and self forces. Force distributions are explored as a function of loop proximity to the boundary of the single crystal model. The deformation of the loop under the influence of these force distributions is computed using a Galerkin variational energy method, and the equilibrium geometry is determined. Additionally, the deformation of a Frank-Reed (FR) source in a single crystal model under the influence of image forces, applied stress, and Peierls forces with varying screw/edge mobility ratios is determined. The results indicate that image forces play a significant role in dislocation force distributions and deformation to a depth from the surface, which is proportional to the loop radius. Large out-of-plane image force distributions on closed loops in "oblique" slip plane/free surface orientations are verified. These forces act in such a way as to repel loop motion from the intersection of the slip plane with the free surface, while causing deformation through the mechanism of cross-slip. Expansion or contraction of shear loops is found to be dependent on the critical applied stress, the radius of curvature, and the proximity/orientation of the loop with respect to the boundary.

[1] TRW Space and Electronics,
Defense Systems Division,
Redondo Beach, CA

[2] Mechanical and Aerospace Engineering Department
University of California, Los Angeles, CA 90095-1597

1 Introduction

Dislocation interaction with free surfaces is of great importance in the understanding of a number of phenomena, which govern the mechanical response of materials to applied loads. For example, the interaction between dislocations and free surfaces plays a significant role in fatigue behavior. In single crystals it is widely accepted that surface roughness caused by the formation of persistent slip bands (PSBs) is the dominant contributing factor to fatigue crack initiation [Rosenbloom and Laird(1993); Repetto and Ortiz(1997); Basinski, Pascual, and Basinski(1983)]. This surface roughness is characterized by the protrusion and extrusion of slip planes due to the effects of dislocation motion and their interaction with free surfaces. Fatigue crack nucleation often accounts for a large portion of the fatigue life of a component. Computer models which simulate the surface roughening of various kinds of single crystals due to random slip on primary slip planes have accurately predicted the number of cycles required for crack nucleation [Repetto and Ortiz(1997); Basinski, Pascual, and Basinski(1983)]. The importance of dislocation motion and free surface interaction is also now being recognized in the field of microscale tribology with respect to MEMS components. A micromechanical dislocation model of frictional slip between two asperities presented by Hurtado and Kim (1999) suggests that slip between two asperities is assisted by the nucleation and gliding of a dislocation loop. This model assumes that the dislocation is nucleated along the perimeter of the contacting regions. For the dislocation to glide, the resultant forces influencing its motion; namely self forces, image forces, and applied forces, must overcome the Peierls barrier. For resultant forces that are directed inwards, the loop will contract

as it glides across the contact area and self annihilates. The end result is the slip of the upper asperity over the lower asperity by a distance of one Burgers vector. Additionally, the interaction between threading dislocations and free surfaces of a strained layer bonded to a substrate plays a significant role in the estimation of the critical thickness of a strained layer for a particular mismatch strain. Misfit dislocations in epitaxially grown thin films are known to be detrimental to the electronic properties of these materials [Beltz and Freund (1993)]. Verdier, Fivel and Groma (1998) have modeled dislocation dynamics at the mesoscale for the indentation test on a Copper crystal. Their work details the effect of image forces developed by a free surface through the use of the finite element technique. Through these examples, the importance of the interaction between dislocations and free surfaces can be clearly established.

In this work, we develop an iterative Finite Element / Dislocation Dynamics method for investigation of the influence of surface forces on dislocation loop stability and motion in finite, three-dimensional crystals. The internal elastic field, forces and motion of dislocation loops are all computed by the Parametric Dislocation Dynamics methodology, developed in Ghoniem and Sun (1999) and Ghoniem, Tong and Sun (2000). Tractions are computed on all crystal surfaces, and a superposition technique is developed, where the tractions are reversed on a crystal of the same configuration, but without dislocations, and the Finite Element Method (FEM) is used to determine the residual stress field, and hence image forces. Since FEM computations are intensive, several accuracy criteria are imposed to determine the rate of image forces re-calculation, as dislocation loops approach the crystal surface. Within one time interval of FEM evaluation, the dislocation loop shape is updated by an implicit time-integration scheme. Several computational techniques for locating dislocation line nodes, and estimation of acting image-type Peach-Koehler forces will be discussed. The motion, deformation and interaction of dislocation loops with crystal surfaces will also be analyzed in this paper. Results of computer simulations will be discussed in terms of the mechanism by which dislocation loops and Frank-Read sources emerge from within the crystal as they approach its surface.

Using the finite element method and the method of Dislocation Dynamics described above, various force distributions on a single shear loop in a BCC Fe single crystal will be determined. The analysis proceeds in the following fashion. First, the displacement, elastic stress and traction fields on the surface of the single crystal model are computed using the Parametric DD method. Then, stress iso-surfaces for the elastic stress field and the field produced by the superposition of the elastic field and the image stress field are calculated and compared to verify that the free surface boundary condition was satisfied. To verify the accuracy of the numerical model, all forces on the loop in the (101)-[111] slip system are computed and compared to distributions proposed in the literature. Having completed this process successfully, loops will then be placed at different locations within the crystal to study the effects of loop/boundary orientation on the various force distributions. Also, the deformation of a single loop will be determined for orientations in close proximity to the boundary. A final analysis will explore the deformation of the dynamics of a Frank-Reed (FR) source in BCC materials with high (10 to 1) and low (2 to 1) ratios of screw to edge Peierls threshold forces.

The paper is organized as follows. First, a brief outline of the theoretical framework of Parametric Dislocation Dynamics (PDD) is given in subsection (2.1), together with details of the computational methods devised for coupling the PDD with the FEM technique in subsection (2.2). Results of our computer simulations are then presented in subsection (3.1) for the elastic field of a single shear loop in a finite isotropic crystal, where we discuss conditions for its equilibrium. In subsection (3.2), we also present results for the equilibrium of FR dislocation sources near surfaces, and analyze the forces acting on them. Finally, a summary and conclusions are given in section (4).

2 Computational Method

2.1 A Brief Description of Parametric Dislocation Dynamics

Ghoniem, Huang and Wang (2001) obtained a differential form of the stress tensor σ, that can be numerically integrated, as given by:

$$\frac{d\sigma}{d\omega} = \frac{\mu V|\mathbf{T}|}{4\pi(1-\nu)R^2}\left\{\left(\mathbf{g}^1\otimes\mathbf{g}_1+\mathbf{g}_1\otimes\mathbf{g}^1\right)+ \right.$$
$$\left.(1-\nu)\left(\mathbf{g}^2\otimes\mathbf{g}_2+\mathbf{g}_2\otimes\mathbf{g}^2\right)-\left(3\mathbf{g}_1\otimes\mathbf{g}_1+\mathbf{I}\right)\right\} \quad (1)$$

Where the three covariant unit vectors: $\mathbf{g}_1, \mathbf{g}_2,$ and $\mathbf{g}_3$ represent the non-orthonornmal set: the unit vector along the direction between a source and a field point (radius vector), the unit tangent vector, and a normalized unit Burgers vector, respectively. The vectors $\mathbf{g}^1, \mathbf{g}^2,$ and $\mathbf{g}^3$ are their contravariant reciprocals, and V is the volume spanned by them. In Eqn. 1, μ = shear modulus, ν = Poisson's ratio, the unit second order tensor = $\mathbf{I}$ is , the magnitude of the tangent vector to a parametric dislocation segment = $|\mathbf{T}|$, and the magnitude of the radius vector = R. The location of any point on the segment is described by the scalar parameter ω, and the total field is obtained as a fast sum over quadrature points on all the segments of a dislocation loop [Ghoniem and Sun (1999)]. The Peach-Koehler force on any loop is obtained by performing a line integral over the segment of the vector: $\mathbf{f}_{PK} = \sigma \cdot \mathbf{b} \times \mathbf{t}$. A variational form of the governing equation of motion of a single dislocation loop has been developed by Ghoniem, Tong and Sun (2000), as :

$$\int_{\Gamma} \left(f_k^t - B_{\alpha k} V_{\alpha} \right) \delta r_k \, |d\mathbf{s}| = 0 \tag{2}$$

Where f_k^t is the k^{th} component of the resultant force, consisting of following types of forces: Peach-Koehler force f_{PK}, the self-force, and the Osmotic force [Hirth and Lothe(1982)], and $\mathbf{s}$ is the arc length vector along the dislocation line. To simplify the problem, we only consider the mobility $B_{\alpha k}$ to be isotropic, i.e. $B_{\alpha k} = B\delta_{\alpha k}$. Let's now define the following dimensionless parameters:

$$r^* = \frac{r}{a}, \qquad f^* = \frac{f}{\mu a}, \qquad t^* = \frac{\mu t}{B}$$

as the dimensionless distance, force and time, respectively. Here, a is the lattice constant, and t is time. Hence Eqn. (2) can be rewritten in matrix form as:

$$\int_{\Gamma^*} \delta \mathbf{r}^{*\top} \left(\mathbf{f}^* - \frac{\mathbf{dr}^*}{dt^*} \right) |d\mathbf{s}^*| = 0 \tag{3}$$

Where, $\mathbf{f}^* = [f_1^*, f_2^*, f_3^*]^\top$, and $\mathbf{r}^* = [r_1^*, r_2^*, r_3^*]^\top$. Following Ghoniem, Tong, and Sun (2000) the dislocation loop can be divided into N_s segments. In each segments, we can choose a set of generalized coordinates q_m at the two ends of each segment j, which can be parametrically described as:

$$\mathbf{r}^* = \mathbf{CQ} \tag{4}$$

Where, $\mathbf{C} = [C_1(\omega), C_2(\omega), ..., C_m(\omega)]$, $C_i(\omega), (i = 1, 2, ...m)$ are shape functions dependent on the parameter ω ($0 \leq \omega \leq 1$), and $\mathbf{Q} = [q_1, q_2, ..., q_m]^\top$, q_i is the generalized coordinate. Substituting Eqn. (4) into Eqn. (3), we obtain:

$$\sum_{j=1}^{N_s} \int_{\Gamma_j} \delta \mathbf{Q}^\top \left(\mathbf{C}^\top \mathbf{f}^* - \mathbf{C}^\top \mathbf{C} \frac{d\mathbf{Q}}{dt^*} \right) |d\mathbf{s}| = 0 \tag{5}$$

Now Let,

$$\mathbf{f}_j \equiv \int_{\Gamma_j} \mathbf{C}^\top \mathbf{f}^* \, |ds| , \qquad \mathbf{k}_j \equiv \int_{\Gamma_j} \mathbf{C}^\top \mathbf{C} \, |d\mathbf{s}| ,$$

and

$$\mathbf{F} = \sum_{j=1}^{N_s} \mathbf{f}_j, \qquad \mathbf{K} = \sum_{j=1}^{N_s} \mathbf{k}_j,$$

then, from Eqn. (5), we finally obtain:

$$\mathbf{K} \frac{d\mathbf{Q}}{dt^*} = \mathbf{F} \tag{6}$$

Eqn. (6) represents a set of ordinary differential equations, which describe the motion of a dislocation loop as an evolutionary dynamical system. In our computer simulations, we use cubic spline as shape functions for dislocation segments, i.e.

$$\mathbf{C} = [2\omega^3 - 3\omega^2 + 1, \omega^3 - 2\omega^2 + \omega, -2\omega^3 + 3\omega^2, \omega^3 - \omega^2]$$

$$\mathbf{Q} = [\mathbf{P}_1, \mathbf{T}_1, \mathbf{P}_2, \mathbf{T}_2]^\top$$

Here, $\mathbf{P}_i$ and $\mathbf{T}_i$ $(i = 1, 2)$ are corresponding position and tangent vectors, respectively. The resulting equations of motion are solved by implicit integration in the PDD computer code: UC-MICROPLASTICITY, and then the results are coupled with the FEM technique to satisfy the boundary conditions, as described below.

2.2 *Coupling between the DD and FEM Computational Procedures*

In the present model, a tensile stress is imposed on a cubic single crystal and its effect on the dislocation loop forces is calculated through the use of the Peach-Kohler formula. To evaluate image stresses due to crystal surfaces, first the elastic stress field in an infinite medium

resulting from the dislocation loop is computed. The tractions that result at the surfaces of the finite crystal from this stress field are then determined, reversed, and placed on the FEM model as boundary conditions. The FEM model is then used to calculate the image stress field. From this stress field, the Peach- Kohler formula can again be used to detrmine image forces on the dislocation loop. This procedure follows the approach of Van der Giessen and Needleman (1995), and extends it to 3-D DD applications.

Having described the general idea behind the coupled FEM-DD approach to the solution of the problem of a single dislocation loop in a finite crystal with external boundary conditions, we will now turn our attention to the details of the calculational method. The elastic field developed by the dislocation loop is evaluated at crystal spatial nodal positions defined by the FEM model of the ANSYS computer program. For the bulk of the present analyses, 10 divisions per cube side were employed for the FEM model. This resulted in 1,331 nodes and 3,990 degrees of freedom. Some analyses were run with a finer mesh generated by using 20 divisions per cube side, thus resulting in 9,261 nodes and 27,780 degrees of freedom. These FEM models have one node in the center of the crystal model with all degrees of freedom constrained to prevent rigid body motion. Once the ANSYS model is created, the coordinates of the nodes and the associated unit normals are introduced into UC-MICROPLASTICITY. Tractions are then calculated, with the unit normal vectors at the surface of the cell. The tractions, with their directions reversed, are then imported into the ANSYS computer program. After the FEM analysis is run and the stress field in the crystal interior computed to an intermediate file, which is then re-written into a format usable by UC-MICROPLASTICITY. The Peach-Kohler formula is then used to calculate the image forces on the loop nodes. Because the FEM analysis only calculates the stress field at specific positions, the stress on the loop nodes has to be estimated by a three-dimensional linear interpolation algorithm [Cook (1995)]. To this end, a number of subroutines were developed to perform the linear interpolation of the stress tensor components from FEM nodal positions to loop nodal positions. These subroutines determine the FEM field nodes that are closest to a specific loop node, and estimate the stress on the loop node by using a linear interpolation method described below.

Loop Node Stress Tensor Estimation

To estimate the stress on a specific loop node, the stress on the nearest FEM field points surrounding the loop node must be found. These field node values are found by comparing the FEM field node coordinate values to the loop node in question. The eight field nodes in a quadrilateral brick element closest to the loop node are thus selected. Another subroutine organizes the stress values and position coordinates so that the loop nodal stresses can be determined by appropriate weighting factors. The procedure used for estimating the stress on loop nodes from the stress that was calculated at the field nodes is taken from an extension of the quadratic quadrilateral used in finite element analysis, into three dimensions [Cook(1995)]. The shape functions are given below.

$$N_1 = [(a-x)(b-y)(c-z)]/8V_e \quad (7)$$
$$N_2 = [(a+x)(b-y)(c-z)]/8V_e \quad (8)$$
$$N_3 = [(a-x)(b+y)(c-z)]/8V_e \quad (9)$$
$$N_4 = [(a+x)(b+y)(c-z)]/8V_e \quad (10)$$
$$N_5 = [(a-x)(b-y)(c+z)]/8V_e \quad (11)$$
$$N_6 = [(a+x)(b-y)(c+z)]/8V_e \quad (12)$$
$$N_7 = [(a-x)(b+y)(c+z)]/8V_e \quad (13)$$
$$N_8 = [(a+x)(b+y)(c+z)]/8V_e \quad (14)$$

In Eqns. 7-14, a, b and c are equal to half the length of a quadrilateral brick element, and V_e is the element volume. The variables x, y and z are the coordinates of the loop node with respect to element's local origin. The stress on the loop node is estimated through the following summation:

$$\sigma_{loop\,node} = \sum_{i=1}^{8} N_i \, \sigma_i \quad (15)$$

Here, N_i is the shape functions and σ_i is the stress on the particular field node. Once the stress on the loop node is established, the image force is calculated using the Peach-Kohler equation. The applied stress is calculated in a similar fashion to that of the image force, and is then entered into UC-MICROPLASTICITY.

Peierls Forces

The applied resolved shear stress required to overcome the lattice resistance to movement by a dislocation loop is referred to as the Peierls-Nabarro stress. This stress is a consequence of the inter-atomic forces/displacement interaction between the dislocation loop and the surrounding crystal. This resistance to dislocation movement is due to the periodic variation in the misfit energy of atomic half planes above and below the slip plane with the dislocation loop. For high dislocation densities, the influence of the Peierls stress on the dynamics of the dislocation loop is comparable to the long-range interactions between the dislocation loops themselves. For low dislocation densities however, the contribution of the Peierls stress is significant. It is generally accepted that the Peierls stress is a dominant controlling factor in the plastic slip of BCC metals at low temperatures [Teodosiu (1982)]. Peierls and Nabarro calculated the dislocation energy per unit length as a function of position. This energy was found to oscillate with period $|\mathbf{b}|/2$, where $\mathbf{b}$ is the Burgers vector. This maximum value for the energy is given in the following equation.

$$E_p = \frac{\mu b^2}{\pi(1-\nu)} exp\left(\frac{-2\pi w}{b}\right) \tag{16}$$

The Peierls stress is the critical stress required to move a dislocation through the crystal. This is the maximum slope of the energy vs. distance curve, divided by the Burgers vector.

$$\tau_p = \frac{2\mu}{(1-\nu)} \exp\left(\frac{-2\pi w}{b}\right) \tag{17}$$

In Eqns. 16 and 17, and w is the distance between the atoms immediately below the dislocation.

Values for E_p and τ_p are sensitive to the details of inter-atomic bonding. τ_p varies between (10^{-6} to $10^{-5}\mu$) for FCC metals, ($10^{-2}\,\mu$) for covalent crystals, and is somewhere in between for BCC metals. The Peierls stress decreases with increasing temperature and with increasing dislocation width. It is also lower for edge dislocations than screw dislocations [Hirth and Lothe (1982)]. Based on the Peierls stress, the corresponding Peierls force can be found through the inner product of the Peierls stress with the Burgers vector.

The ratio of Fe edge to screw velocities is estimated to be ≈ 2). By assuming that the ratio of Peierls forces associated with edge and screw dislocations are inversely proportional to the velocity ratio, the Peierls force in the direction of the Burgers vector was taken as $\frac{1}{2}$ that in the direction normal to the burgers vector. Other ratios were also explored to determine the variability in the deformed geometry with respect to this variable. The calculation of the Peierls force is given by the following formula.

$$\frac{\mathbf{F}}{L} = \tau_p \left(1 + \sin(\cos^{-1}\{\frac{\mathbf{b}\cdot\mathbf{u}}{|\mathbf{b}|\,|\mathbf{u}|}\}\right) \frac{\mathbf{u}}{|\mathbf{u}|} \tag{18}$$

The stress threshold value, τ_p is taken as ($10^{-3}\mu$) for Fe, $\mathbf{u}$ is the displacement vector, and $\mathbf{b}$ is the Burgers vector.

3 Results for Dislocation Interaction with Free Surfaces

3.1 A Shear Loop in a Finite Crystal

The displacement field for a shear dislocation loop with a radius of 4000 a is shown in the vector plot of Fig. 1. The stress field of the loop in an infinite crystal was calculated first by UC-MICROPLASTICITY, and the corresponding reversed tractions necessary for solving the FEM boundary value problem determined, as can be seen in Fig. 2. The stress iso-surfaces formed by the σ_{xx} stress component of the elastic stress field is added to the stress field formed by surface image stresses, and the results are shown in Fig. 3. The superposition of the image stress field onto the elastic stress field of the dislocation loop results in a total stress field with no normal components at the (x = 10,000 a) surface, as can be clearly seen in Fig. 3. The stress iso-surface appears to be repelled from the surface. These results, along with similar results for the shear components, show that the free surface boundary condition has been satisfied.

Force Distributions

Force distributions on a 4000 a-radius shear loop in the (101)- [111] slip system of an Fe single crystal with an applied load of 100 MPa were calculated. The applied, image, Peierls, self and resultant force distributions are all shown Fig. 4 below. The image, self and Peierls force distributions are all on the shear plane, while the applied and resultant force distributions are characterized by large out-of-plane components. The distribution of the applied force on the circular shear loop is similar to that proposed by Kroupa(1966).

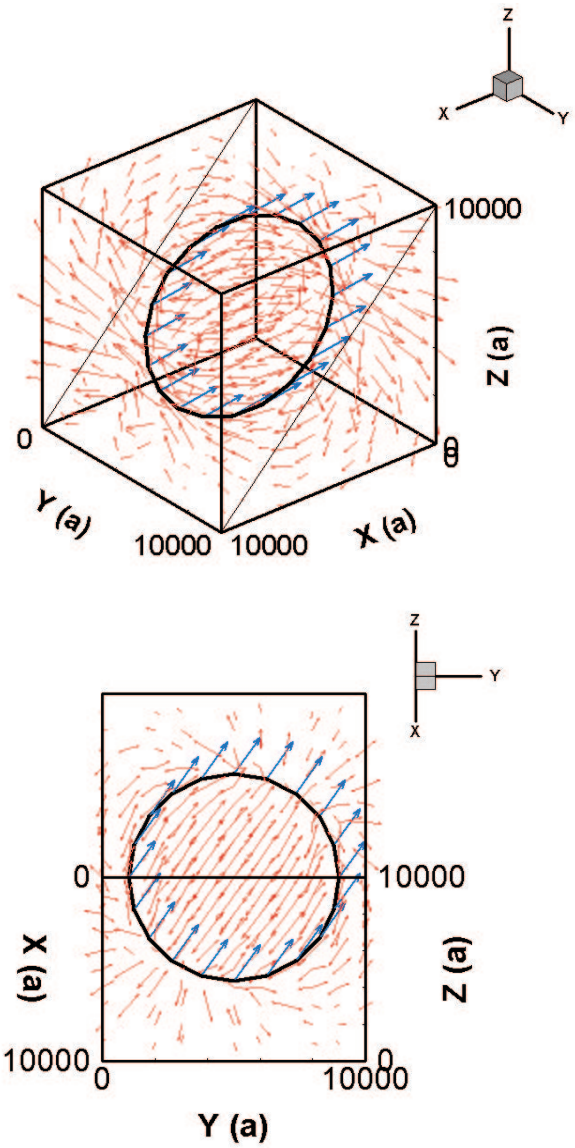

Figure 1 : Two views of the displacement field induced by a 4000 a-radius shear loop in the (101)-[111] slip system. Burgers vectors are represented at loop nodes.

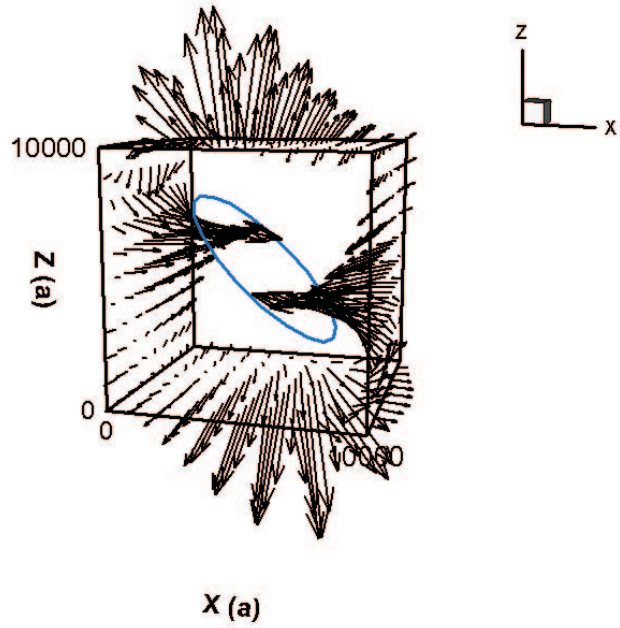

Figure 2 : Vector plot for the tractions produced by the elastic stress field of a 4000 a radius shear loop

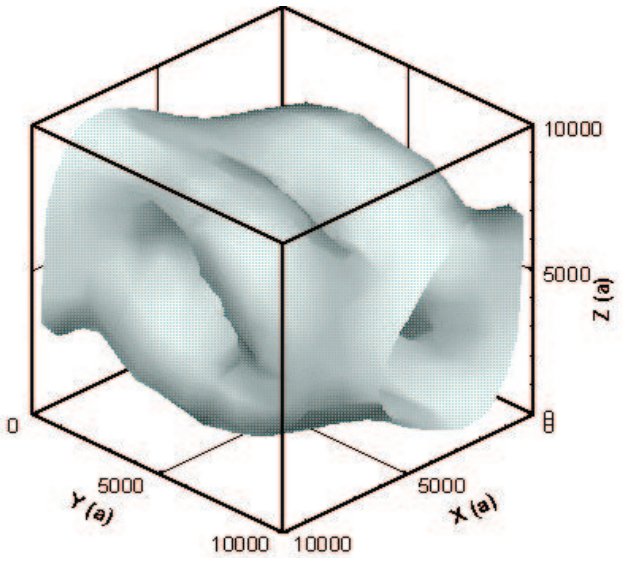

Figure 3 : $\sigma_{xx} = 2000$ MPa stress iso-surface for the total dislocation plus image elastic field

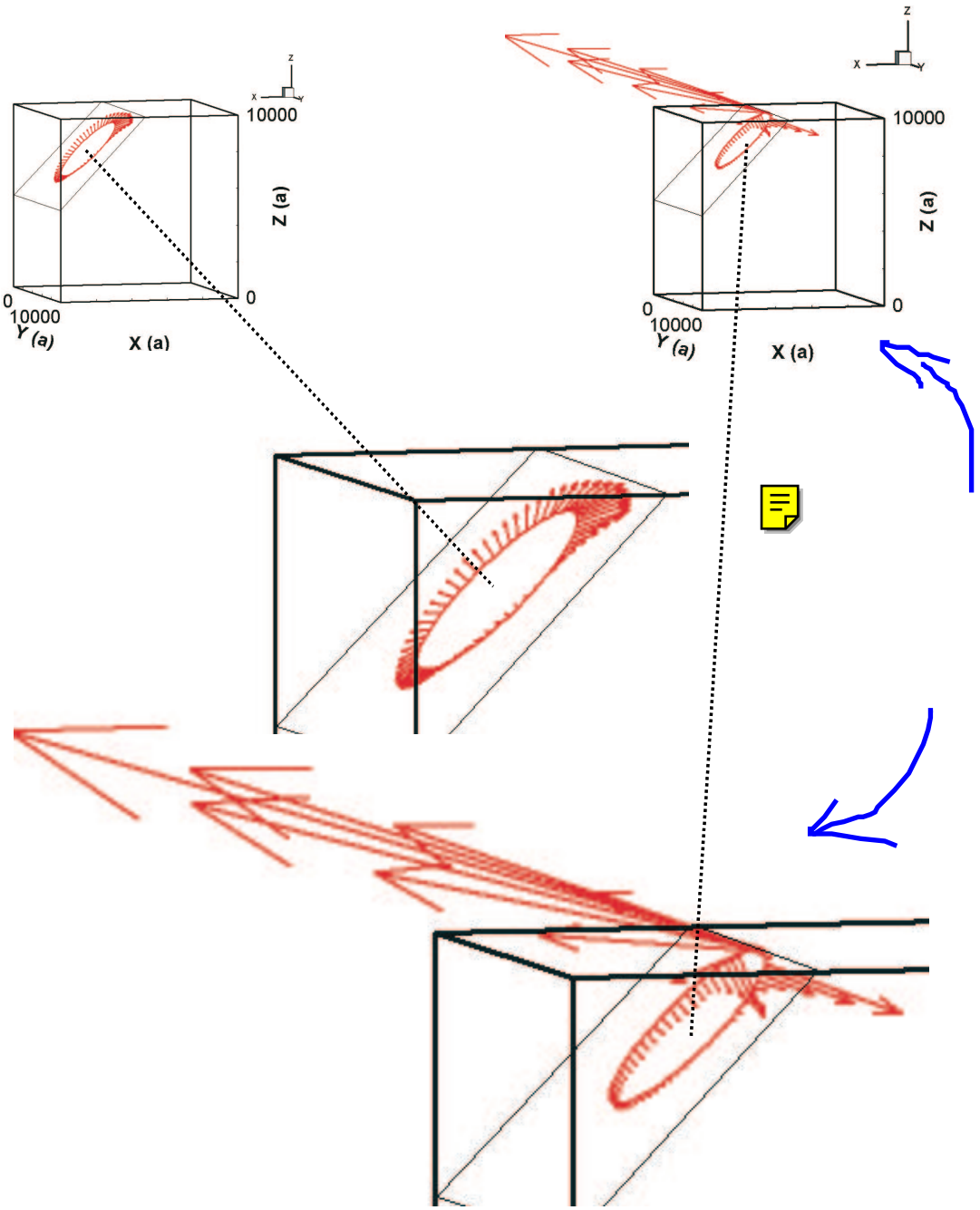

Figure 4 : Force distributions on a 4000 *a* radius shear loop in the (101)-[111] slip system in Fe, applied stress σ_{xx} = 100 MPa. Vectors to scale except self and image with scale factors of 2 and 10, respectively

Self forces seek to increase the length of screw components and decrease the length of edge components as a consequence of total energy minimization for the loop. The screw orientation has a lower energy per unit length as compared to the edge component, and hence is "stiffer" in opposing applied forces. Peierls forces are larger in the direction perpendicular to the Burgers vector, resulting in low mobility of the screw component as opposed to the edge component of the loop. Dislocation loops in BCC metals thus tend to have long, straight screw components, especially at lower temperatures.

Equilibrium of Shear Loops Near Crystal Surfaces

To complete the analysis of the influence of free crystal surfaces, a single dislocation loop was placed at different positions within the single crystal model, and the force distributions were calculated. In addition to loop position, other variables were evaluated including loop diameter, applied stress magnitude, and the number of FEM degrees of freedom. For all analyses, the material modelled is BCC Fe ($\mu = 36.4\ GPa, \nu = 0.25$, and $a = 0.285\ nm$). An analysis was conducted with a fine mesh of 20 divisions per side and 60 nodes per loop. The loop is placed at 250 a from the crystal edge. The results of this analysis are illustrated in Fig. 5. As the loop approaches the crystal corner, image forces increase, and on the portion of the loop closest to the boundary, they are characterized by attractive in-plane and attractive out-of-plane components. A deformation analysis was also conducted on this loop/boundary configuration. The results are displayed in Fig. 6. These results indicate that the loop advances away from the corner in the direction of the Burgers vector. It must however be noted that the motion of the loop is limited to the slip plane in the present numerical model. It is also obvious from Fig. 6 that large out-of-plane forces can induce cross-slip.

To better understand the qualitative relationship between the position of the shear loop and the crystal boundary forces, a loop with a radius of 2000 a was placed at different positions with respect to the top crystal surface. As the loop arrives at the surface, the magnitudes of image forces become very large. For a loop very close to the boundary, this force distribution becomes repulsive when projected onto the slip plane, and is characterized by large out-of-plane forces on the portion of the loop closest to the boundary. These forces should promote cross-slip toward the free surface for the screw components. Fig. 7 shows that forces on loop nodes not near the boundary evolve from a radial outward distribution at 250 a from the boundary, to a downward normal (from the slip plane) distribution at a distance of 10 a from the boundary. These results indicate that image force distributions are heavily dependent on the proximity of the loop to the the top crystal surface. Having established the distribution of forces, the deformed shape of the loop under an applied stress of 50 MPa was calculated (see Fig. 8). As predicted by the nodal force distribution, the loop is repelled by the surface due to the influence of image forces, as a result of constraining loop motion to be only on the glide plane. A final equilibrium loop geometry is achieved at a distance of 212 a from the free surface. If the model allowed for motion out of the slip plane, the loop would advance toward the boundary through cross-slip of its screw components. To understand why surface image forces become repulsive at close proximity to the boundary, the surface tractions were compared for this same configuration at 250 a and 10 a from the boundary. These tractions show that there are large shear forces acting on the surface of the crystal, and that these forces grow very large as the loop comes close to the boundary. Thus, the tendency of the loop to move out of its glide plane is driven by surface shear forces.

3.2 The Influence of Crystal Surfaces on the Deformation of Frank Reed Sources

Friedel concluded that a dislocation is attracted towards its image, and that it should arrive perpendicular to the free surface in order to achieve the most stable configuration [Friedel (1964)]. However, a dislocation in a medium that is separated from a free surface by a thin film of thickness h and shear modulus μ' behaves quite differently. A screw dislocation at a depth L from the interface will be drawn toward the free surface if $\mu' < \mu$. It will be repelled however, if $\mu' > \mu$ and $L << h$. For $\mu' > \mu$, and $L >> h$, the dislocation will be attracted toward the surface. This implies that there is an equilibrium position from the surface on the order of the film thickness h from the interface. In ionic crystals such as potassium chloride, evidence supports the conclusion that image forces repel dislocations from breaking the surface. Nabarro also states that the image forces may induce cross slip [Nabarro(1967)]. Gilman and cowork-

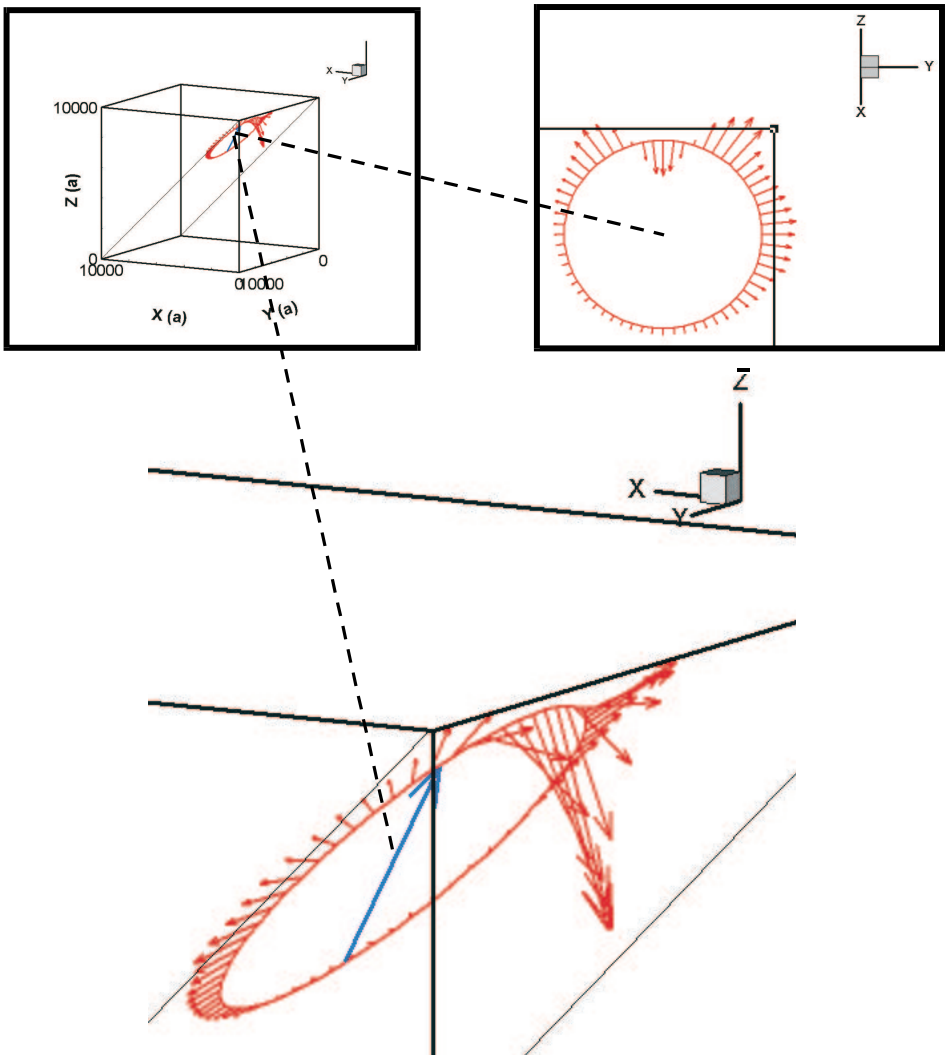

Figure 5 : Two views of the image force distribution on a loop in the corner of the unit cell. The loop is 250 *a* from the edge of the cell. The Burgers vector direction is also represented.

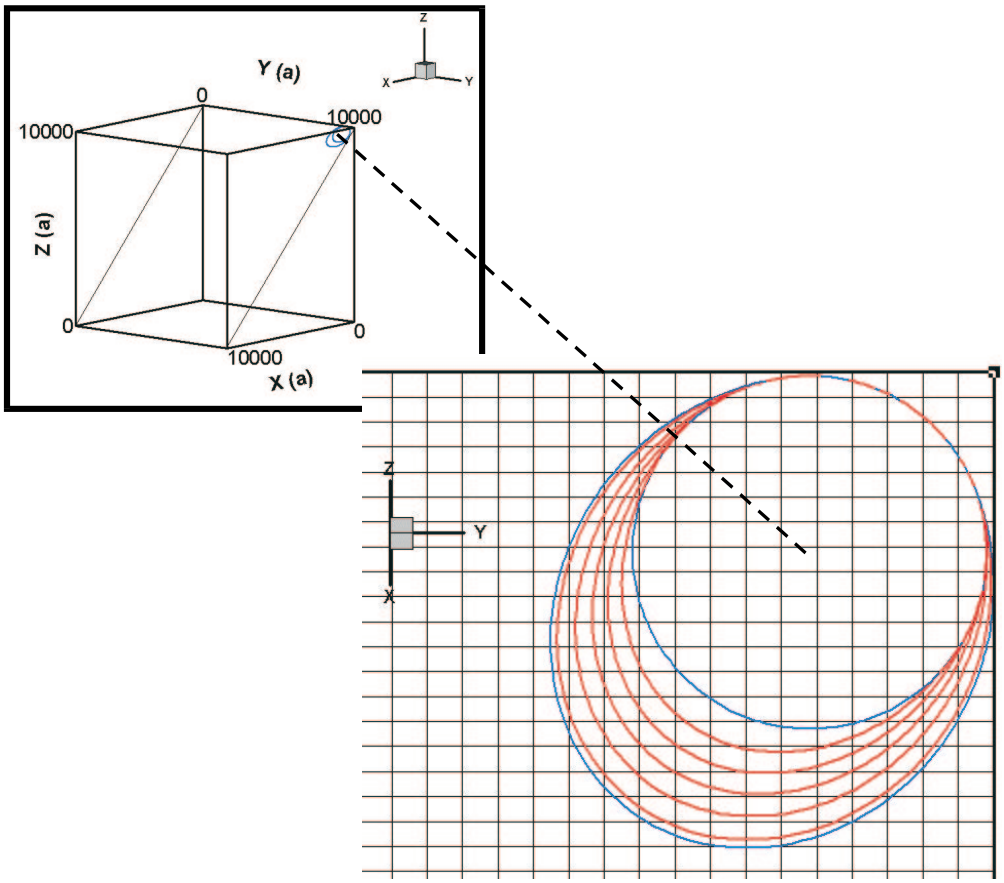

Figure 6 : The 500 *a* radius loop and the deformation that results under an applied stress of 350 MPa.

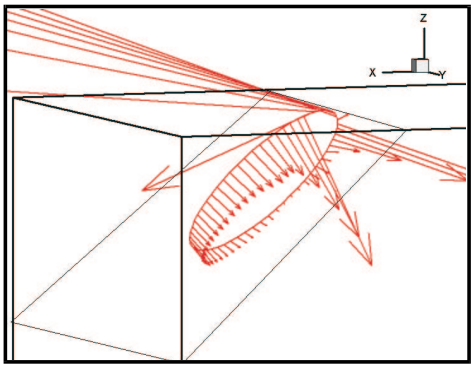

10a from z = 10000a boundary
scale factor = 1

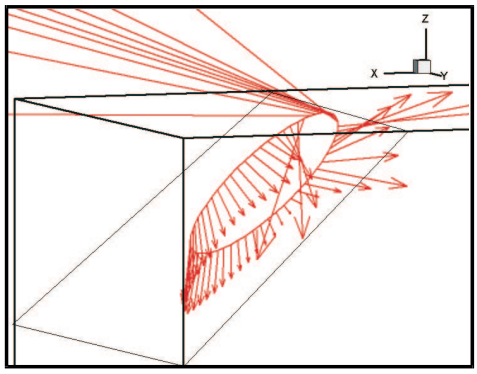

50a from z = 10000a boundary
scale factor = 10

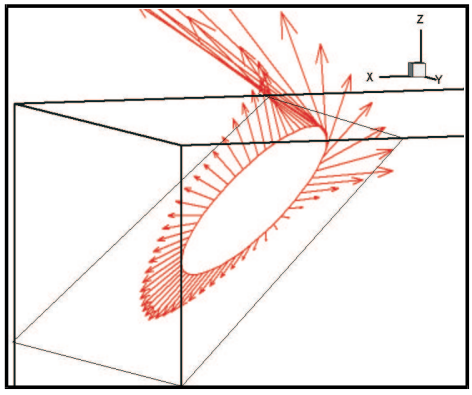

250a from z = 10000a boundary
scale factor = 10

Figure 7 : Image force distributions on a 2000 *a* radius shear loop in the (101)-[111] slip system, (A)1000 *a*, and (B) 10 *a* from z=10000 *a* surface. Vector scale factors: (A)100,(B) 1 .

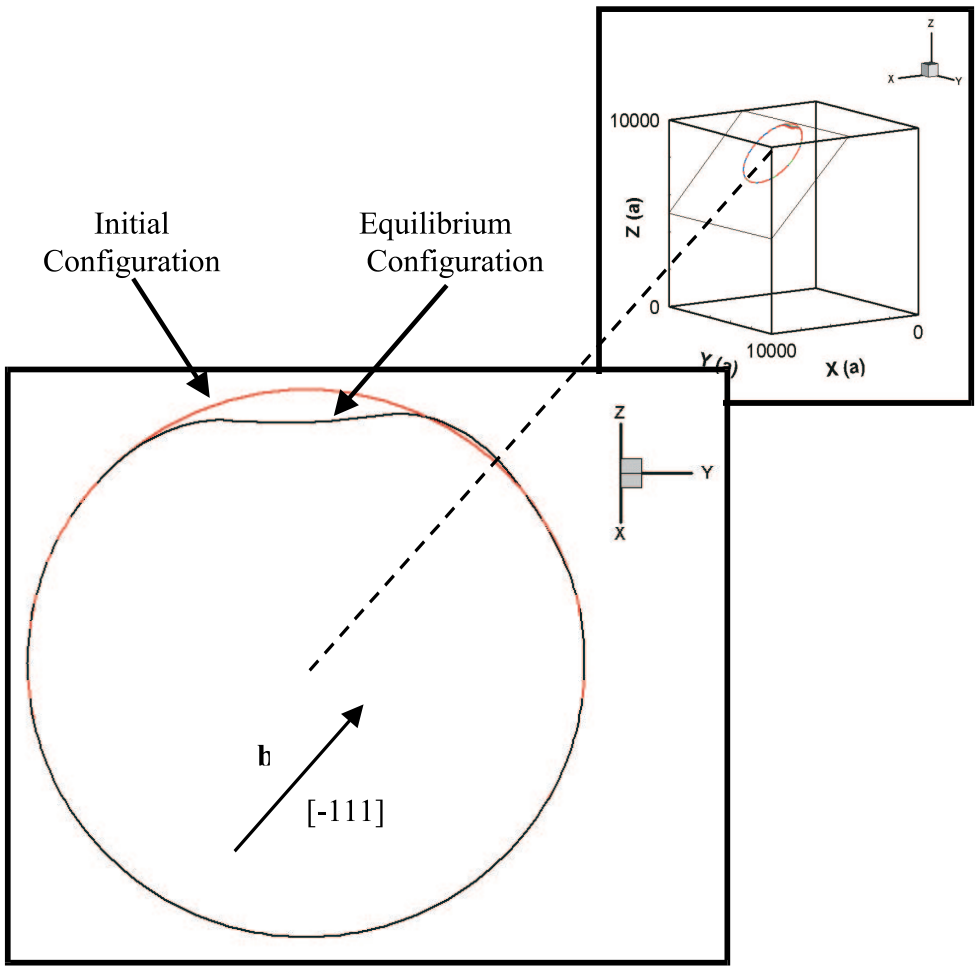

Figure 8 : Deformation of a 2000 *a* radius shear loop in the (101) -[111] slip system. The loop is initially 10 *a* from the surface with applied stress: σ_{xx} = 50 MPa.

ers conducted experimental studies involving the measurement of dislocation velocities in LiF single crystals [Gilman (1961)], and proposed a mechanism of dislocation motion under the influence of surface forces in a single crystal, as schematically illustrated in Fig. 9. In this schematic, a screw dislocation (AB) lies in the

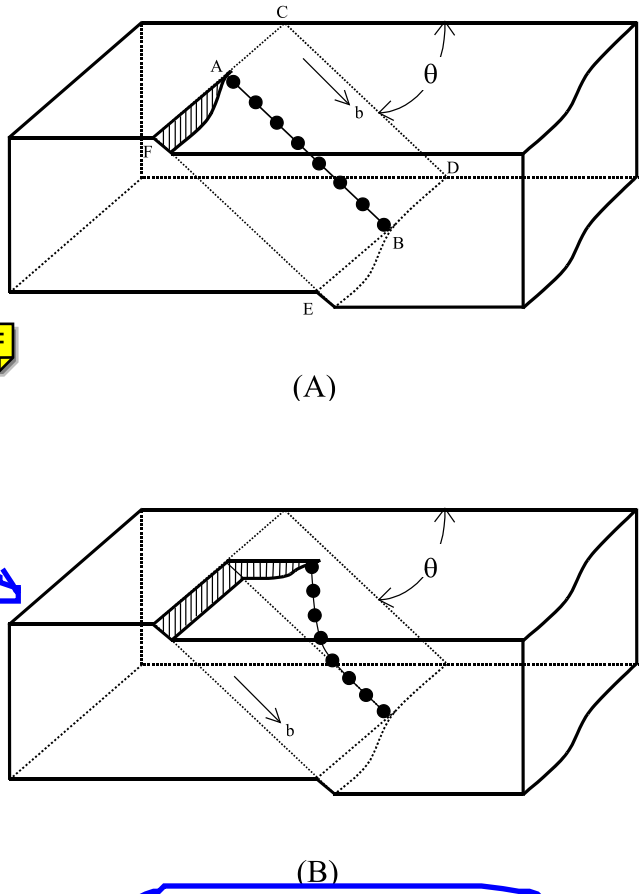

Figure 9: Schematic of cross-slip of a screw dislocation adjacent to a surface in a crystal.(A) Initial configuration, and (B) the deformation of the dislocation line following cross-slip (after [Gilman(1961)]).

glide plane (CDEF), which is at an angle θ with respect to the free surface. Although the dislocation typically would move in the direction of (AC), deformation through cross-slip has been observed [Gilman (1961)]. This mechanism of cross-slip was assumed by Gilman to be the result of energy minimization through the reduction in the length of the dislocation along the slip plane. With the image force distribution observed in Fig. 8, it is obvious that this effect is the result of the large surface shear forces uncovered by the present analysis.

The deformed geometry of a Frank Reed (FR) source in BCC Fe under the influence of an applied stress was then computed to determine the influence of surface image forces on the shape of the FR-source. In Fig. 10, a stress of 125 MPa was applied to a crystal containing a single FR source. The FR source is located on the slip plane with origin at(7500,5000,7500). The local coordinates of the fixed points on the FR-source are (-2000, 3000) and (2000,3000). The equilibrium shape of the FR-source is evolved, as it approaches the free crystal surface. The equilibrium position of the source is approximately 163 a from the surface of the crystal model, as can be seen in Fig. 10.

To study the effects of anisotropic Peierls forces on the deformation of FR-sources, the ratio of edge to screw Peierls forces were varied. Fig. 11 shows the deformation of an FR-source in a finite crystal with a screw to edge Peierls force ratio of 2 to 1, and a Peierls threshold shear stress of $1 \times 10^{-6}\mu$, and an applied stress of 200 MPa. This case may be representative of a crystal with a "low" screw to edge Peierls force ratio, such as an FCC crystal. The results depicted in Fig. 11 also show the deformation of an FR-source in a crystal with a screw to edge Peierls force ratio of 10 to 1, and Peierls shear stress threshold of $10^{-3}\mu$, typical of a BCC crystal and an applied stress of 700 MPa. Both cases indicate that the deformation for the high ratio case evolves with significantly less curvature than for the low ratio case, consistent with the observations of dislocation loop curvatures in FCC and BCC crystals, respectively.

4 Conclusions

The computer modelling and numerical results presented in this paper seek to determine the influence of free surfaces on dislocation motion in metallic single crystals. Much of the work in Dislocation Dynamics that is presented in the literature testifies to the importance of surface effects. However, little if any modelling has been completed which describes the precise nature of force distributions in 3-D geometry induced by the proximity of dislocation loops to crystal surfaces with specified boundary conditions. Based on the results of computer simulations for the elastic fields around static and dynamic dislocation loops and FR-sources in single crystals, and the corresponding forces and deformation of these loops, the following conclusions can be drawn.

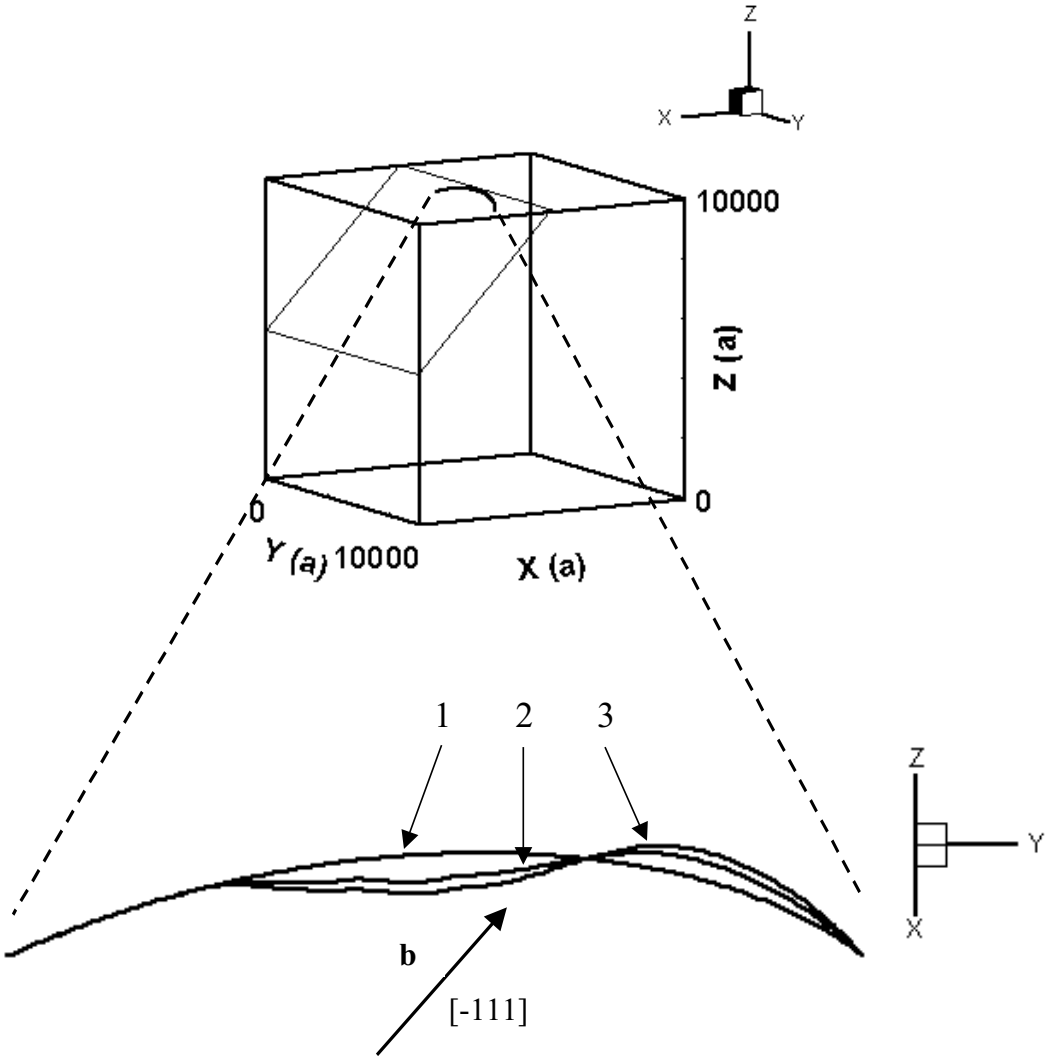

Figure 10 : Isometric view of a crystal containing an FR-source, and a 2-d view of the deformed geometry as viewed normal to the (101)-plane. (1) Initial geometry, (3) is the equilibrium geometry under an applied stress σ_{xx} = 125 MPa.

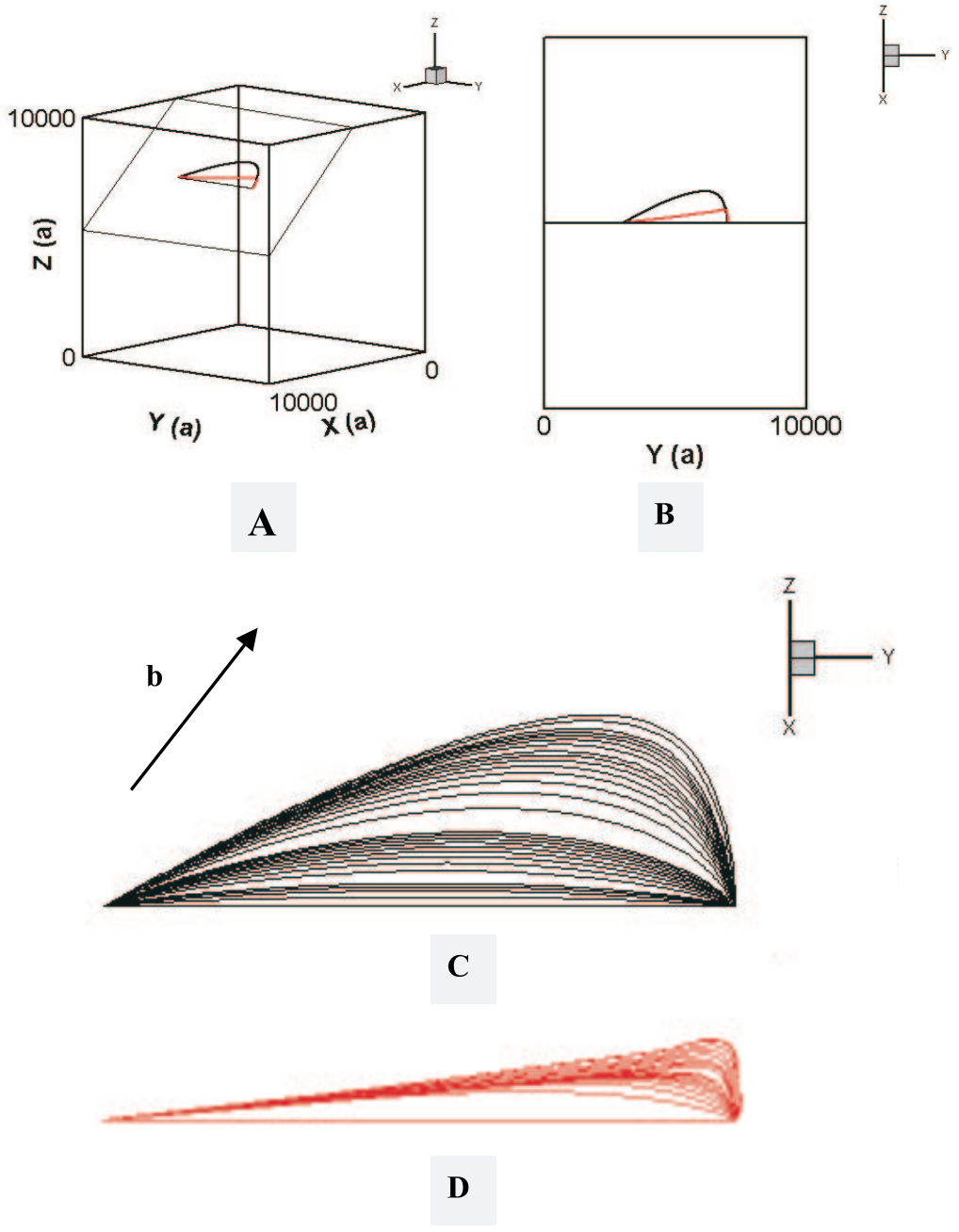

Figure 11 : Isometric (A), and 2-d (B, C, and D) views of the evolution of an FR-source near a crystal surface. View C depicts the "low screw/edge force" ratio case, while D depicts the "high" ratio case. 4000 time steps.

1. Imposed surface traction boundary conditions can be achieved through the use of a hybrid finite element method (FEM), coupled with Dislocation Dynamics (DD). Peierls and self-forces cause the loop to deform preferentially (stretch) in the direction of the Burgers vector, while surface image forces act to either attract or repel the loop, depending on its distance from the boundary, and the orientation of the slip plane with respect to the nearest free surface. For slip planes at an oblique angle to a free surface, the image forces on the closest screw-component portions of the loop are characterized by a large out-of-plane component, which acts to pull the loop toward the surface through the mechanism of cross-slip. For example, for loop model geometry characterized by 20 nodes, and 10 mesh divisions per side in the FEM model, the out of plane component became dominant at approximately 500 lattice constants.

2. For slip planes that are normal to the free surface, image force distributions on dislocation loops have negligible out-of-plane components. These image forces are directed along the slip plane regardless of the distance of the loop from the boundary. Furthermore, these image forces can either attract or repel portions of the loop closest to boundary depending on the distance between the loop and the boundary. For a 4000 lattice parameter diameter loop characterized by a 60 node geometry, and an FEM model with 20 mesh divisions per side, calculated image forces are attractive for a loop/free surface separation of 250 lattice parameters. For the same model, but with a separation of 10 lattice parameters between the loop and the free surface, the image forces are repulsive to the loop segment nearest to the surface.

3. Image forces dominate the resultant force distribution for orientations of the shear loop closest to the free surface. The distance from the boundary at which image forces become significant can be estimated based on the image force/self force ratio. This distance varies with respect to the loop radius. Loops with large radii are affected by image forces deeper into the single crystal than are loops with small radii. For small loops, self forces dominate and cause contraction. Thus, the expansion or contraction of the loop is dependent on a critical applied stress, radius of curvature, and proximity from the boundary.

4. Shear dislocation loops and FR-sources in similar slip systems under similar loading configurations close to the surface deform and evolve into similar geometric shapes. A dislocation loop (radius=2000 a, σ_{xx} = 50 MPa, initial loop surface separation of 10 a) and an FR-source of initial length= 4000 a, σ_{xx} = 150 MPa, initial separation from boundary = 535 a in the "oblique" orientation deform into similar shapes. The loop evolves into an equilibrium position 212 a from the surface, while the FR-source evolves to an equilibrium position approximately 163 a from the free surface.

5. Analysis and comparison of modelling results for FR-source deformation under the influence of an applied stress indicates that dislocation loops in BCC crystals deform into geometry with significantly less curvature than in FCC crystals under the same conditions . For the "low" Pierels ratio, the Peirels threshold was taken as $10^{-6}\mu$. For the "high" Pierels ratio, the Pierels threshold was taken as $10^{-3}\mu$.

Acknowledgement: Research is supported by the US Department of Energy, Office of Fusion Energy, through Grants DE-FG03-98ER54500 and DOE Grant DE-FG03-00ER54594 with UCLA.

References

Basinski, Z.S; Pascual, R.; Basinski, S.J. (1983):Low Amplitude Fatigue of Copper Single Crystals-I. The Role of the Surface in Fatigue Failure. *Acta Metall.*, **31(4)** 591.

Beltz, G.E.; Freund, L.B. (1993): Dislocation Threading Through an Epitaxial Film: An analysis Based on the Peierls-Nabarro Concept. *Materials Research Society Symposium Proceedings*, Volume **308**, Materials Research Society, Pittsburg, Pennsylvania

Cook, R.D. (1995): *Finite Element Modeling for Stress Analysis*, **John Wiley & Sons Inc.**, New York.

Friedel, J. (1964): *Dislocations*, Pergamon press, New York, 1964.

Ghoniem, N.M.; Sun, L. (1999): Fast Sum Method for the Elastic Field of 3-D Dislocation Ensembles, *Phys. Rev. B*, **60(1)** 128.

Ghoniem, N.M; Huang, J.M. (2001): Computer Simulations of Mesoscopic Plastic Deformation with Differential Geometric Forms for the Elastic Field of Parametric Dislocations : Review of Recent Progress, Invited Paper at the 5th Euro-Conference on Mechanics of Materials, Delft, Netherlands, March 6-9, 2001, Also in press *J. de Physique*, in press.

Ghoniem, N.M.; Tong, S.H.; Sun, L.Z. (2000): Parametric Dislocation Dynamics: A Thermodynamcis-based Approach to Investigations of Mesoscopic Plastic Deformation, *Phys. Rev. B*, **B1(1)** 913.

Gilman, J.J (1961): *Phil. Mag.*, Series 8, **6** 159.

Hirth, J.P.; Lothe,J. (1982): *Theory of Dislocations*, 2^{nd} Edn.,**McGraw-Hill**, New York.

Hurtado, J.A.; Kim, K. (1999): Scale Effects in Friction of Single Asperity Con- tacts. I. From Concurrent Slip to Single-Dislocation-Assisted slip, *Proc. R. Soc. Lond.*, **A 455** 3363.

Kroupa, F. (1966): *Theory of Crystal Defects*, edited by B. Gruber (Academia Publishing House, Prague), p.275. 39.

Nabarro, F. (1967): *Theory of Crystal Dislocations*, Clarendon Press, London, 1967.

Repetto, E.A; Ortiz M. (1997): A Micromechanical Model of Cyclic Deformation and Fatigue-Crack Nucleation in F.C.C. Single Crystals. *Acta Mater.*, **45(6)** 2577.

Rosenbloom, S.N.; Laird C. (1993): Fatigue Crack Nucleation Based on a Random Slip Process-I Computer Model. *Acta Metall. Mater.*, **41(12)** 3473.

Teodosiu, C. (1982): *Elastic Models of Crystal Defects*, **Springer-Verlag**, 1982.

Van der Giessen, E.; Needleman, A. (1995): *Model. Simul. Mater. Sci. Eng.* , **3(5)** 689.

Verdier, M.; Fivel, M.; Groma, I. (1998): Mesoscopic scale simulation of Dislocation Dynamics in FCC metals: Principles and Applications. *Model. Simul. Mater. Sci. Eng.*, **6** 755.